Supplementary Material

Architecting Hydrangea-Inspired Nitrogen-Doped Hollow Carbon with Isolated Co Atoms for Superior Oxygen Reduction Catalysis

Xiaolan Gao[a†], Yue Li[b†], Zhiqing Zhang[a], Hao Zhang[b], Ge Li[a*]
[a] Department of Mechanical Engineering, University of Alberta, Edmonton, Alberta, Canada
[b] Department of Chemical and Materials Engineering, University of Alberta, Edmonton, Alberta, Canada
[*] Corresponding author: Prof. Ge Li: ge.li@ualberta.ca

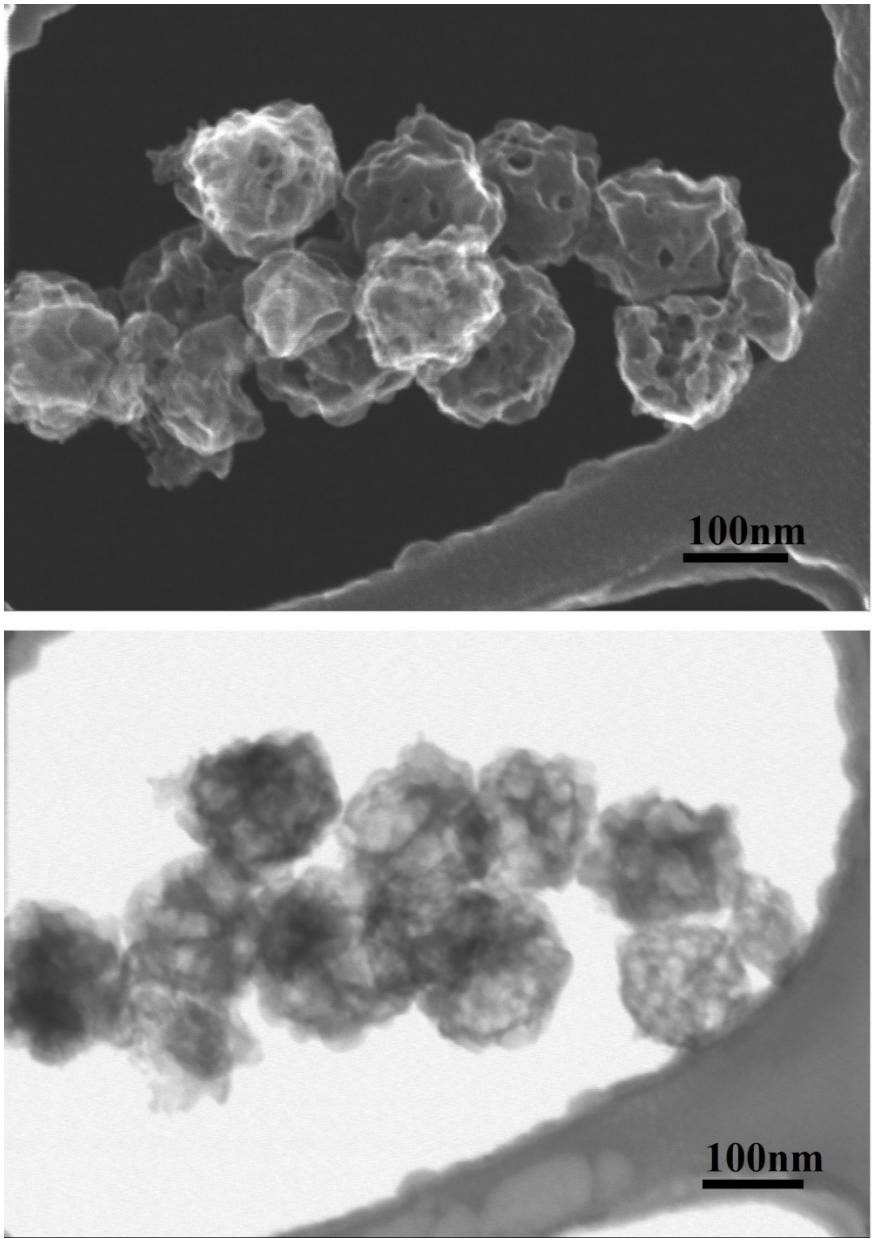

Figure S1. High Resolution Scanning Electron Microscope (HR-SEM) of Co-LC/NC

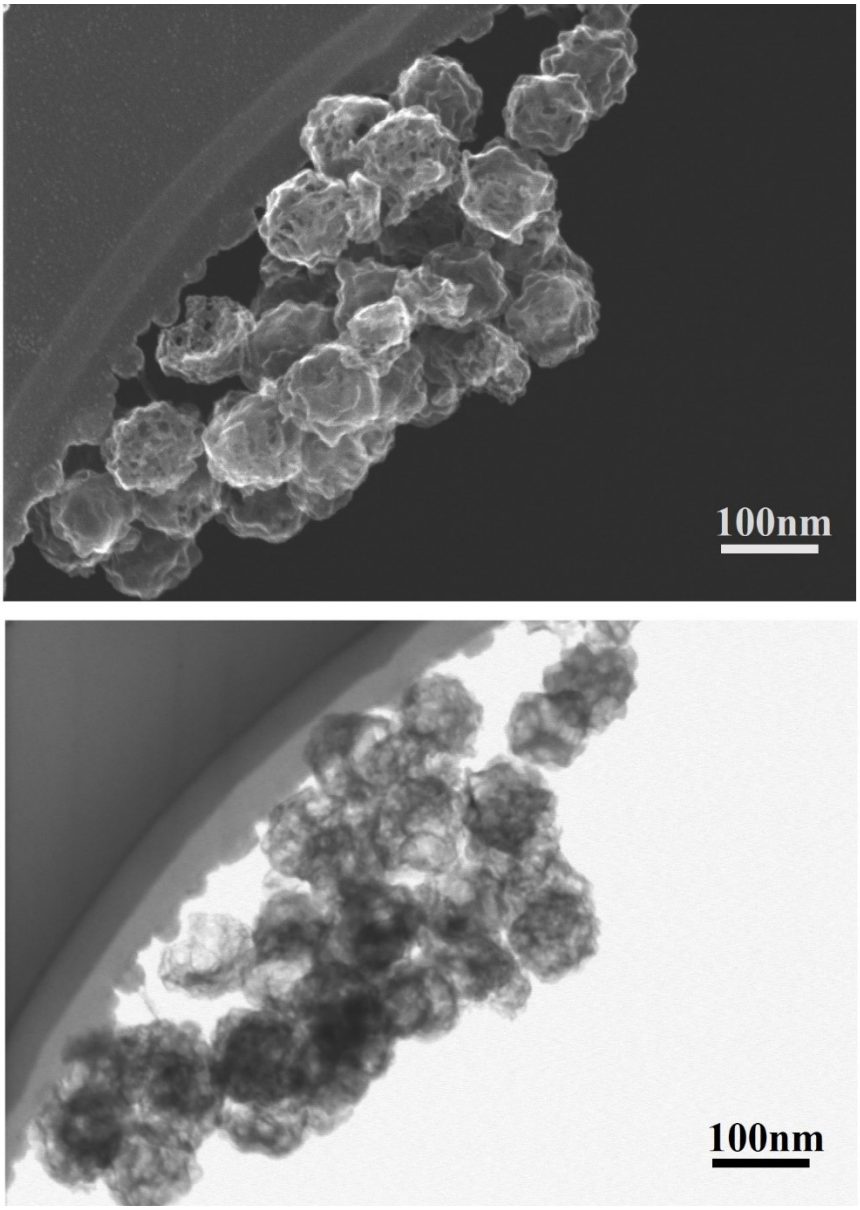

Figure S2. High Resolution Scanning Electron Microscope (HR-SEM) of Co - cluster/NC

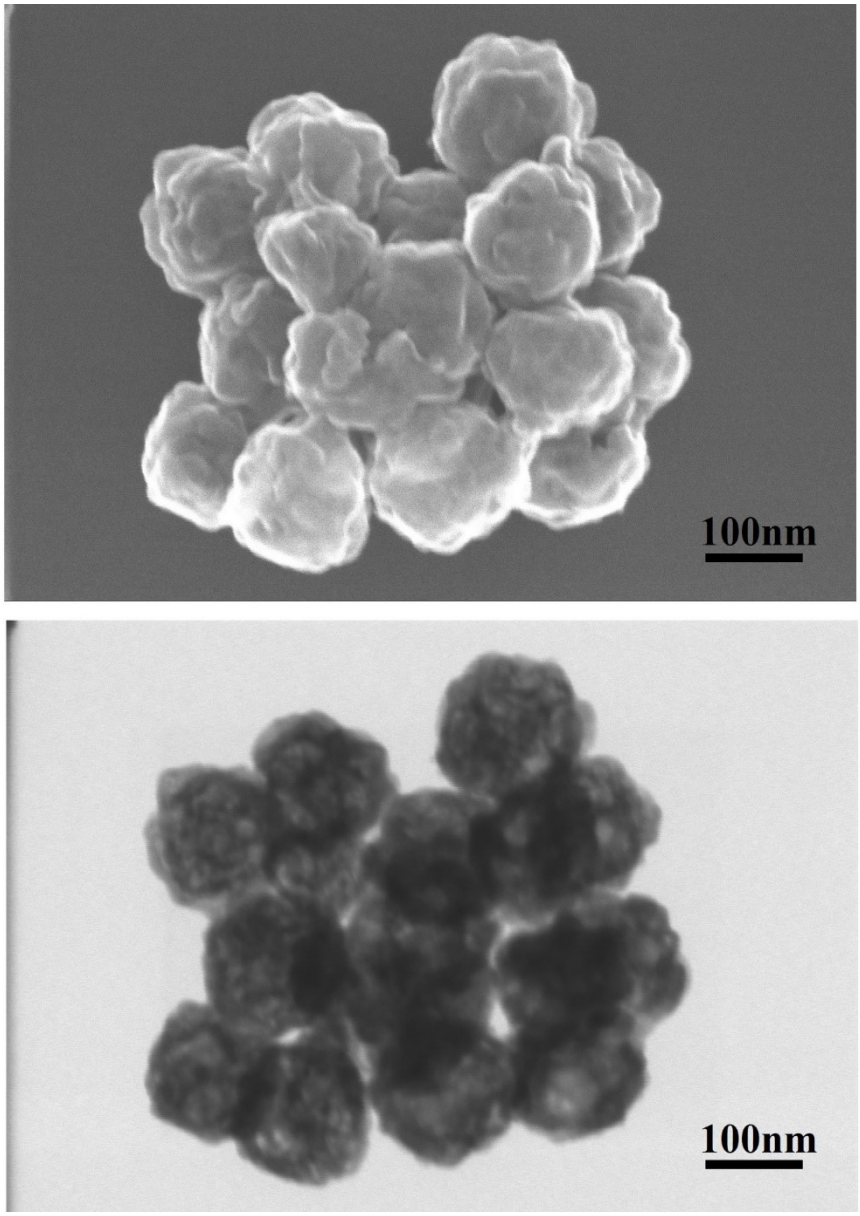

Figure S3. High Resolution Scanning Electron Microscope (HR-SEM) of NC

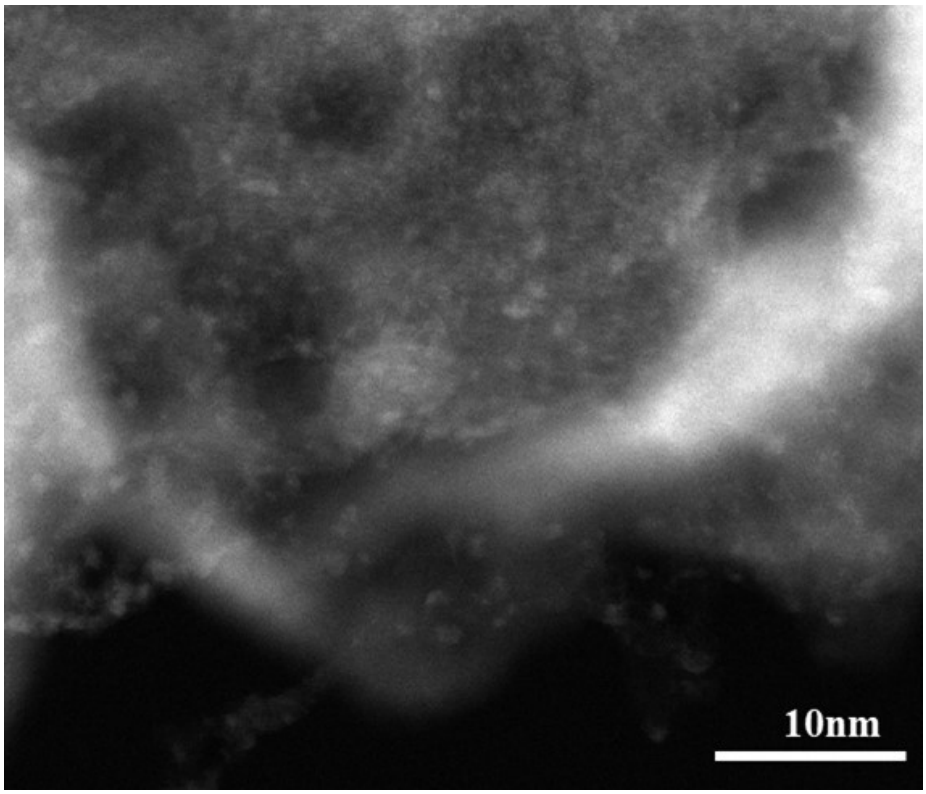

Figure S4. HAADF-STEM image of Co -cluster/NC

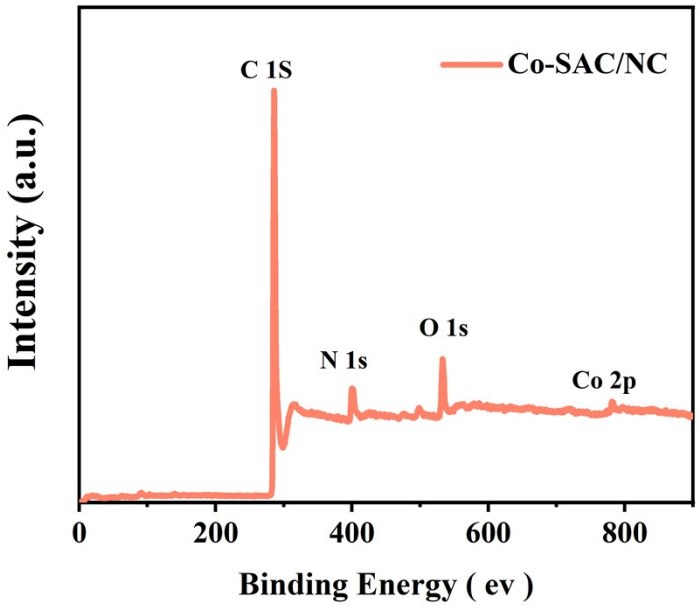

Figure S5. High-resolution XPS of Co -SAC/NC.

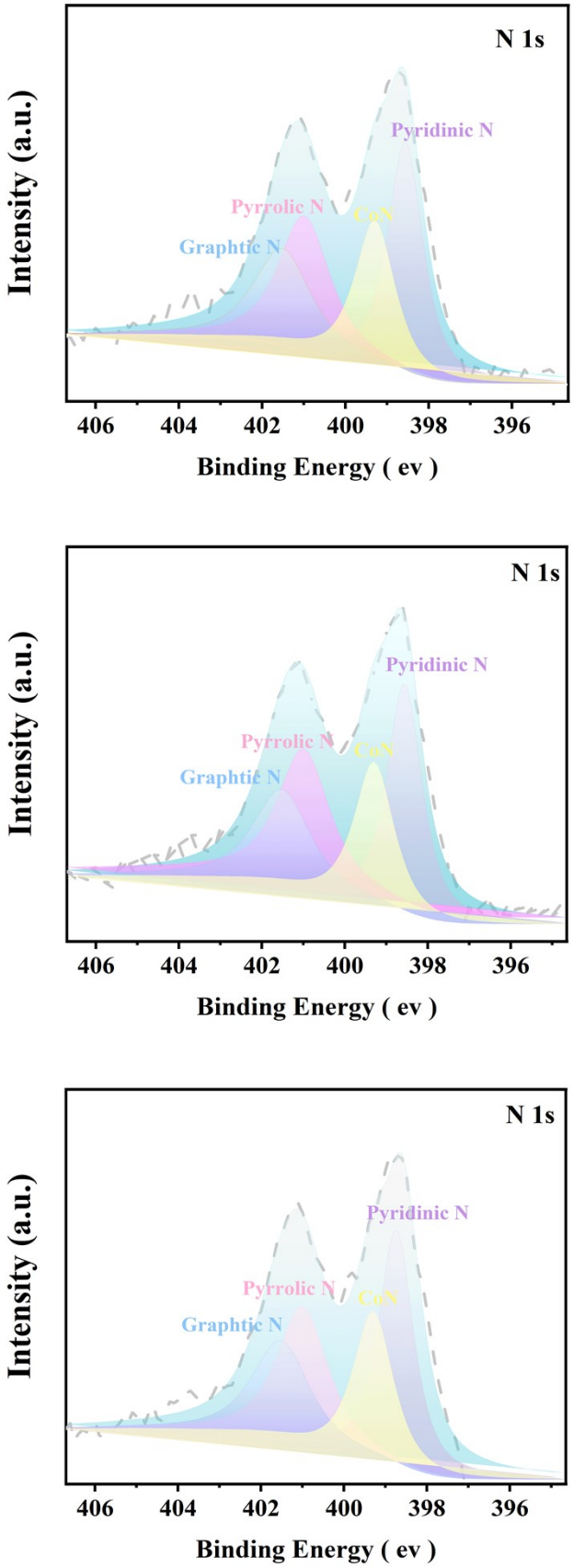

Figure S6. High-resolution XPS of, Co -cluster/NC,Co -LC/NC and NC of N 1s

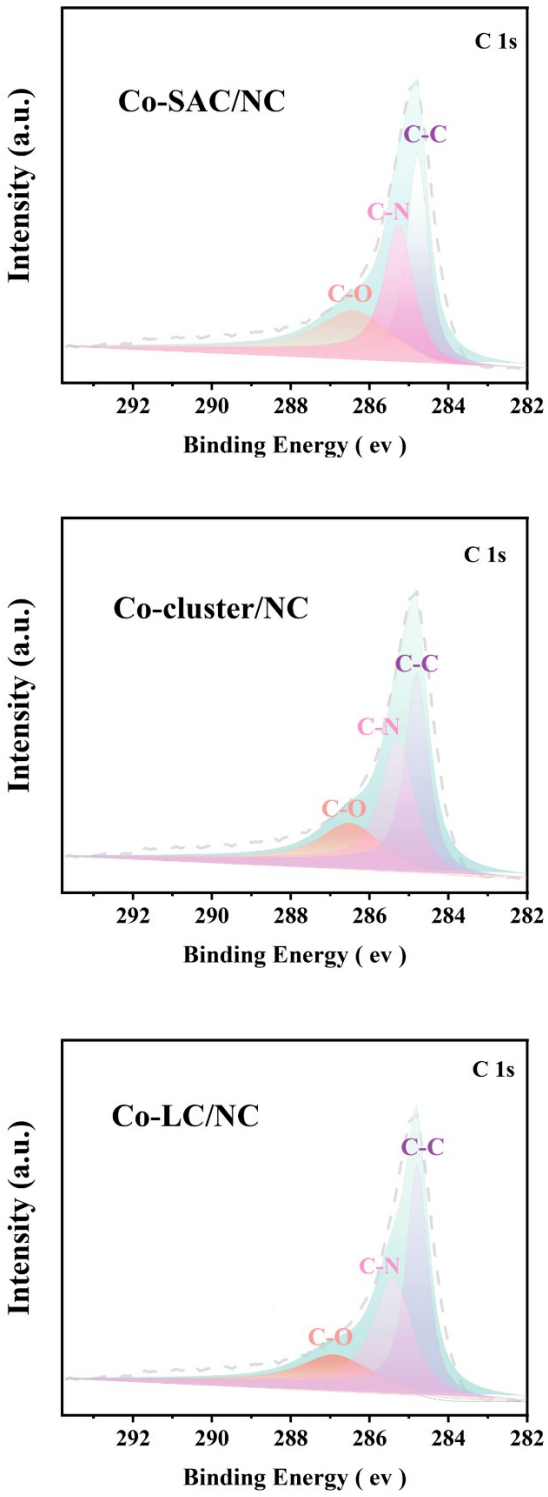

Figure S7. High-resolution XPS of Co -SAC/NC, Co -cluster/NC and Co -LC/NC for C 1s.

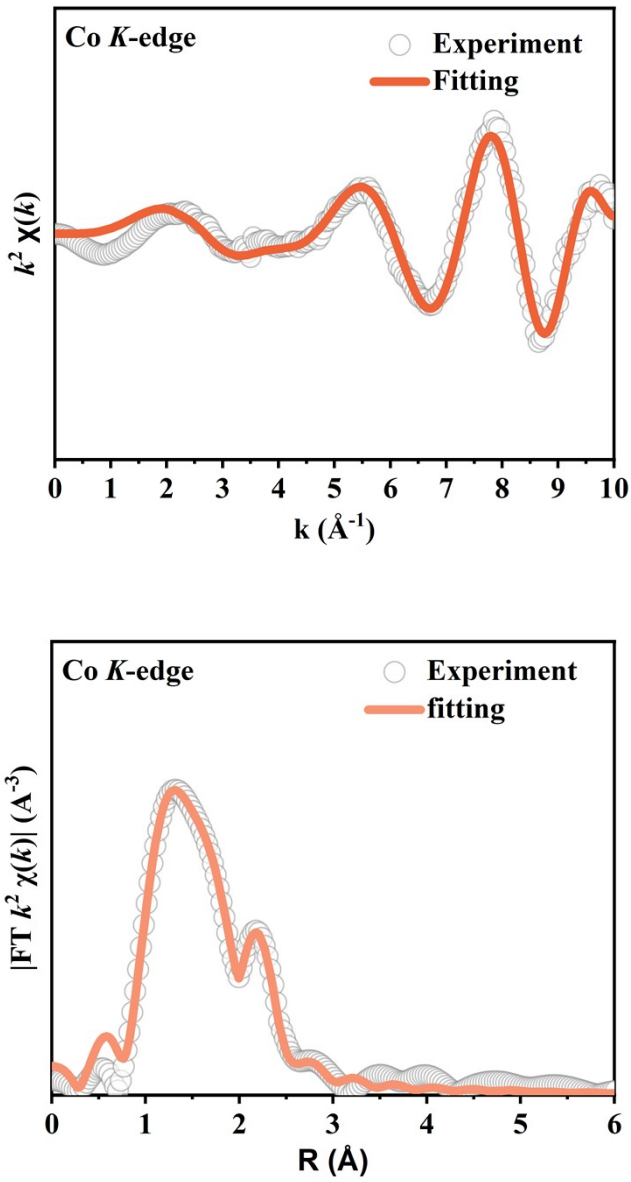

Figure S8. K^3-weighted Co K-edge EXAFS oscillations and FT-EXAFS fitting patterns of Co-cluster/NC.

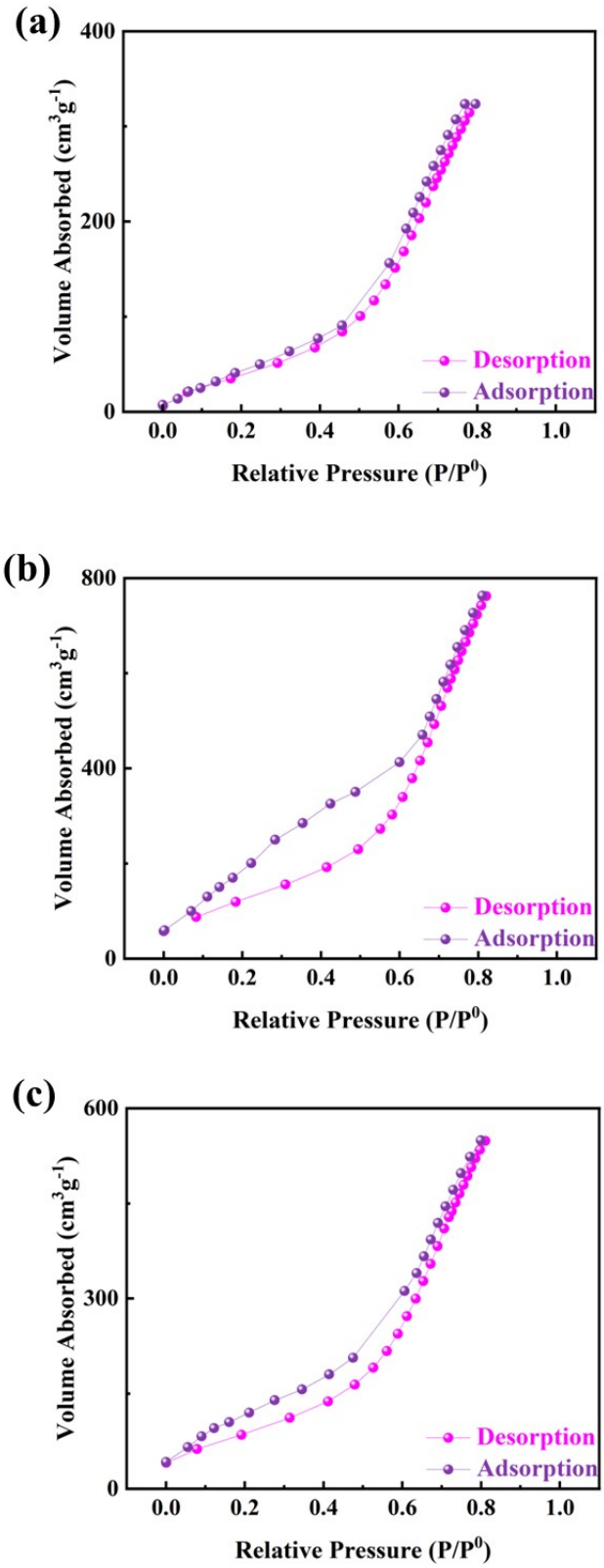

Figure S9. Nitrogen adsorption-desorption isotherms of the as-prepared catalysts (a) Co-SAC/NC (0mg NH_4Cl), (b) Co-SAC/NC (NH_4Cl at 700 ^oC) and (c) Co-SAC/NC (NH_4Cl at 400 ^oC).

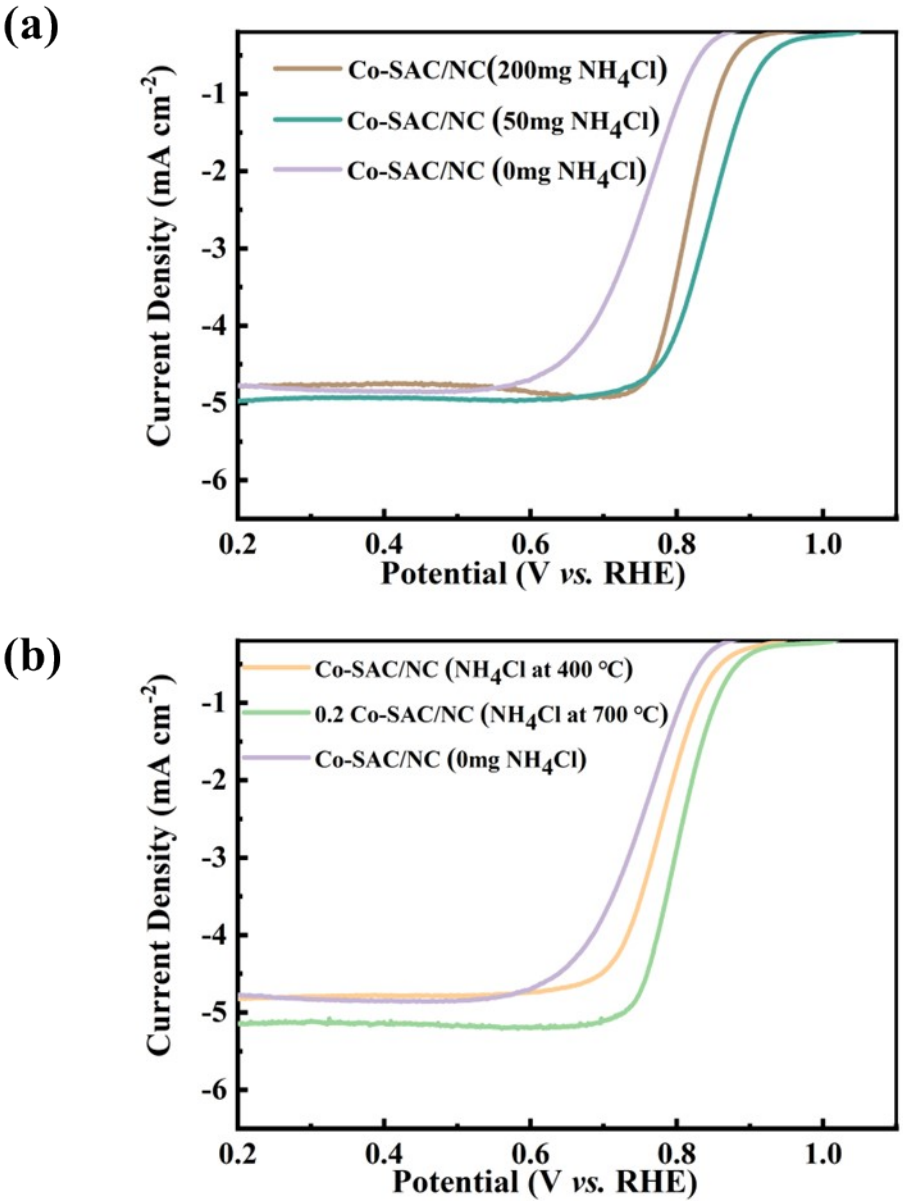

Figure S10. (a) LSV curves of Co-SAC/NC (200mg NH_4Cl), Co-SAC/NC (50mg NH_4Cl) and Co-SAC/NC (0mg NH_4Cl). (b) LSV curves of Co-SAC/NC (NH_4Cl at 400 ^oC), Co-SAC/NC (NH_4Cl at 700 ^oC and Co-SAC/NC (0mg NH_4Cl).

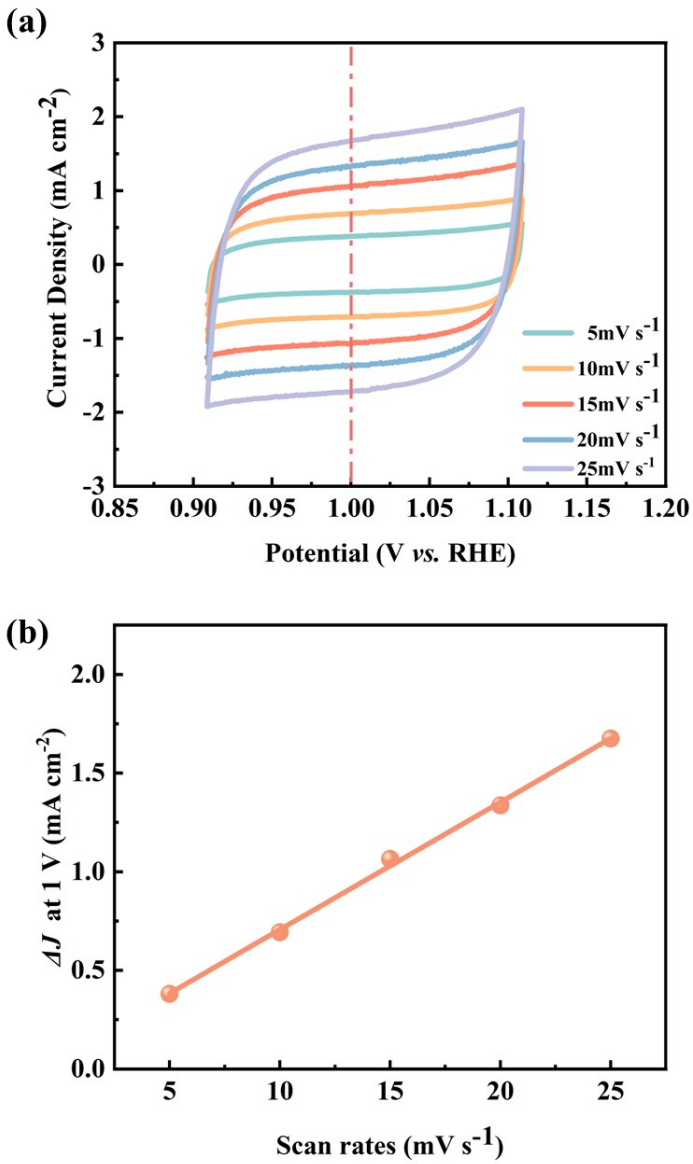

Figure S11. (a)The CV curves of Co-SAC/NC at different scan rates from 5mVs^{-1} to 25mVs^{-1}. (b) The half of current density variation ($\Delta J = (J_a - J_c)/2$) at 1 V plotted against scan rate.

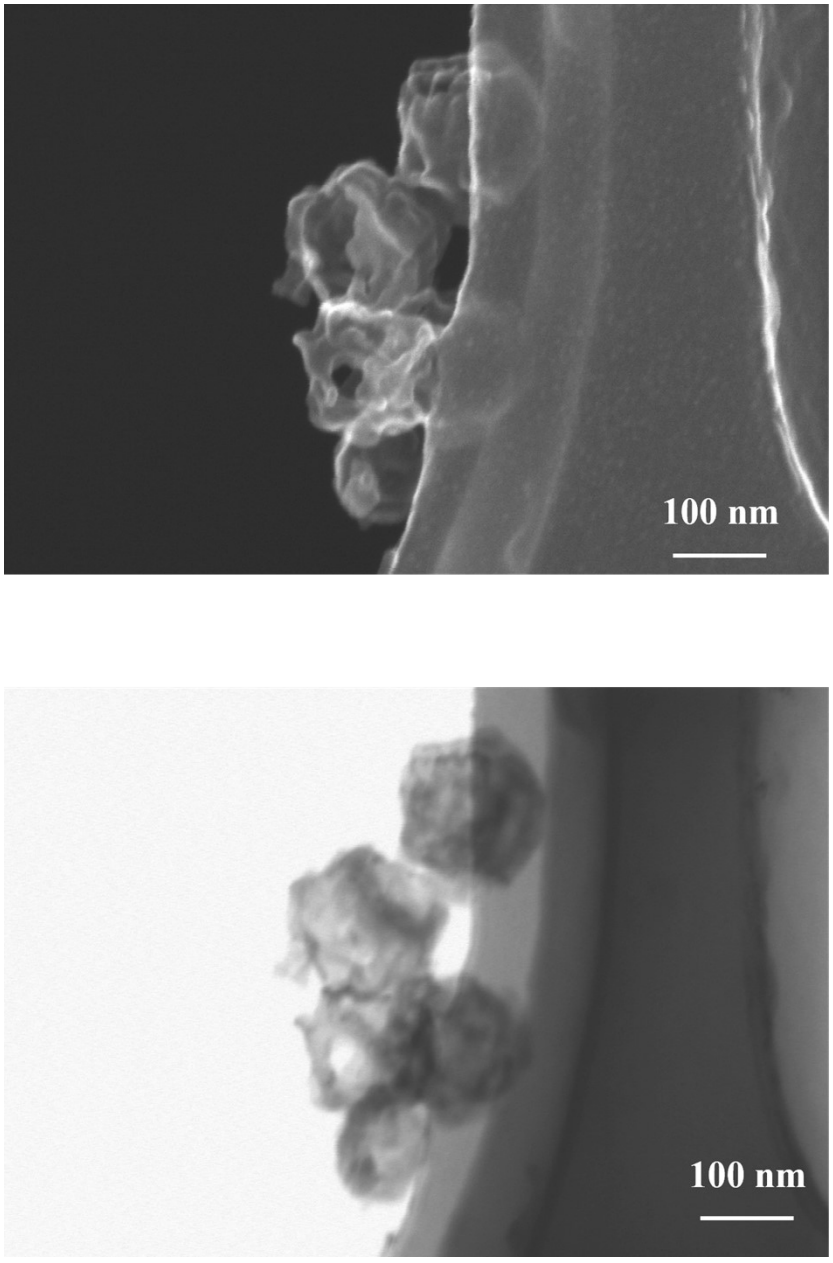

Figure S12.HR-SEM of Co-SAC/NC after cycling.

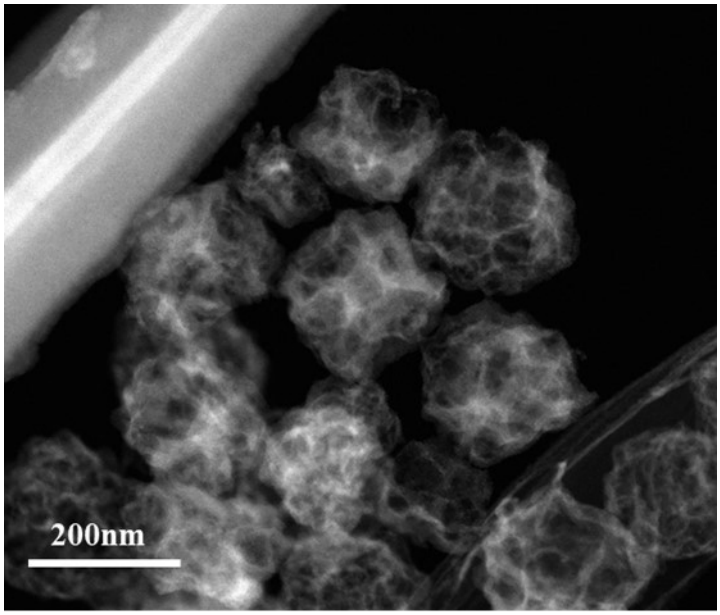

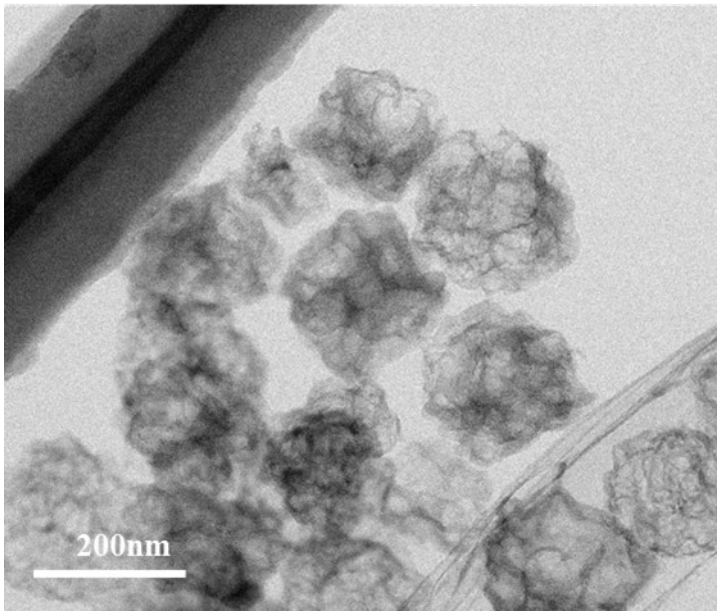

Figure S13.HR-STEM of Co-SAC/NC after cycling.

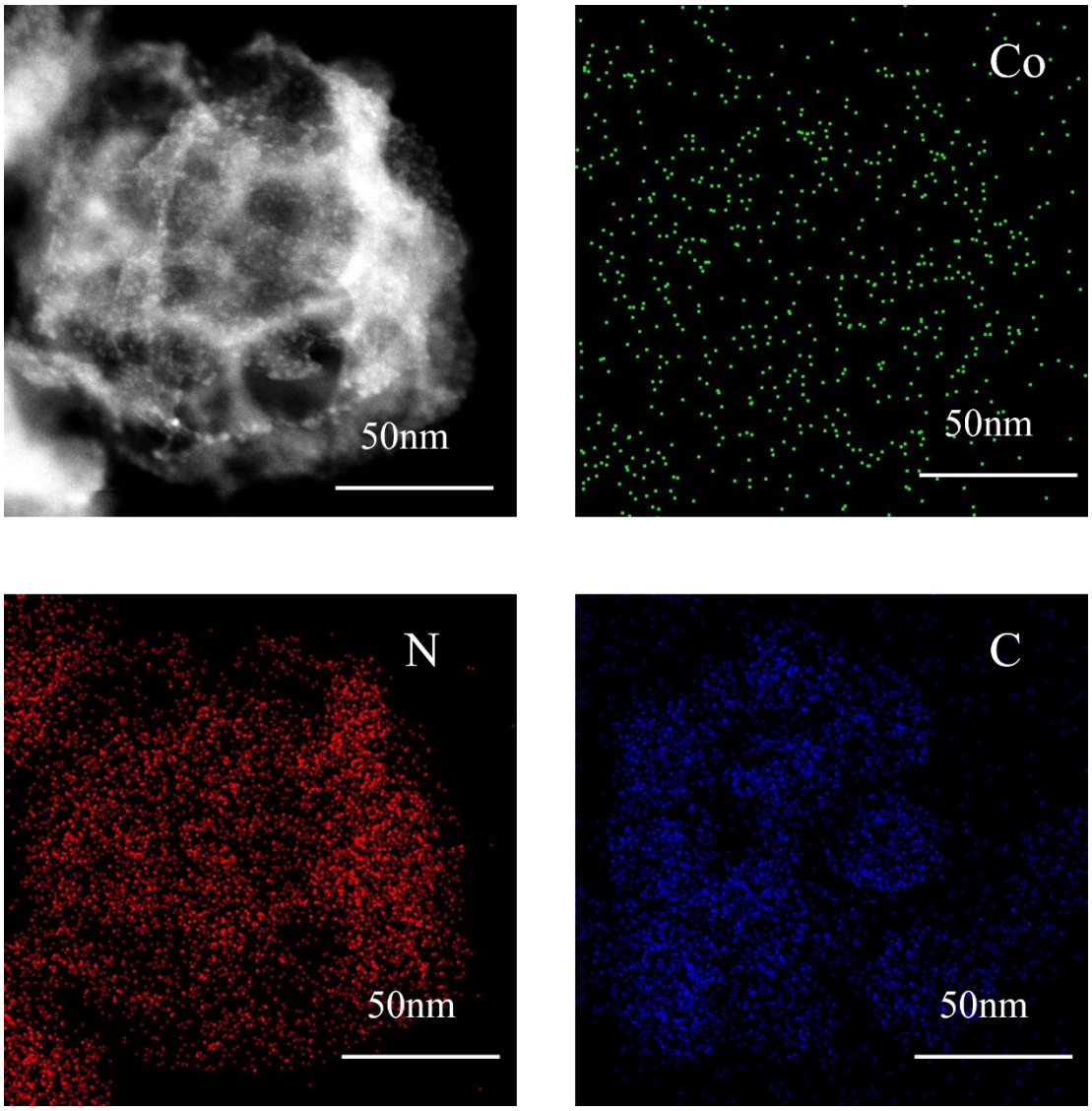

Figure S14. EDS elemental mappings of Co-SAC/NC after cycling.

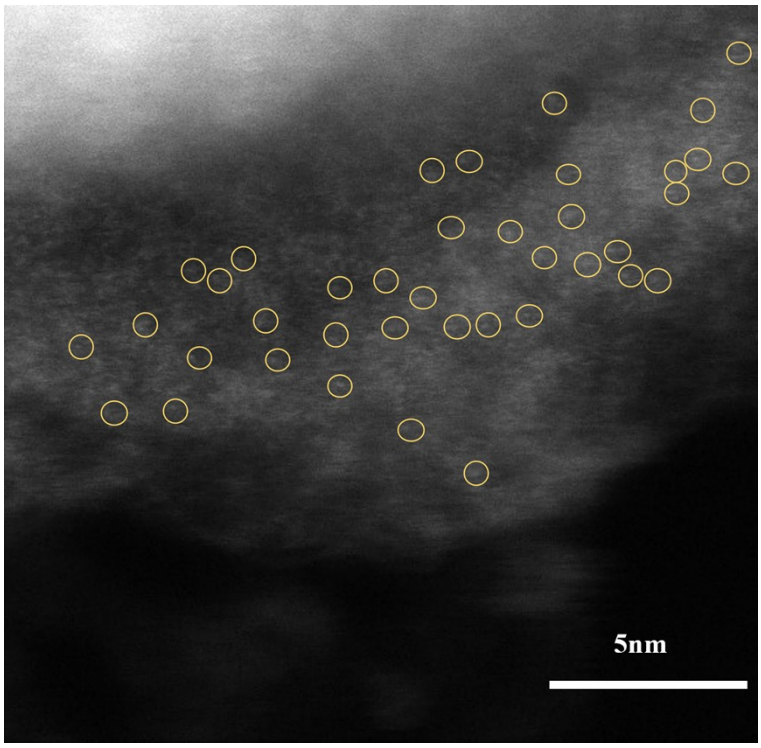

Figure S15. Aberration-corrected HAADF-STEM images

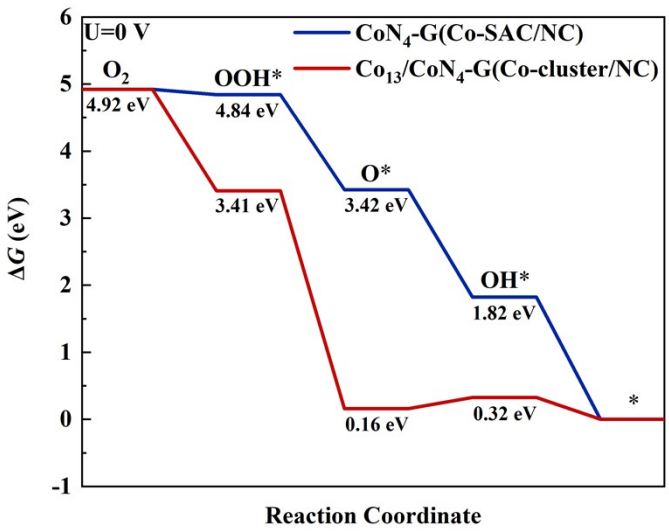

Figure S16. (a) Calculated free energy diagrams of ORR at pH = 13 and U = 0 V for Co single atom and cluster anchoring.

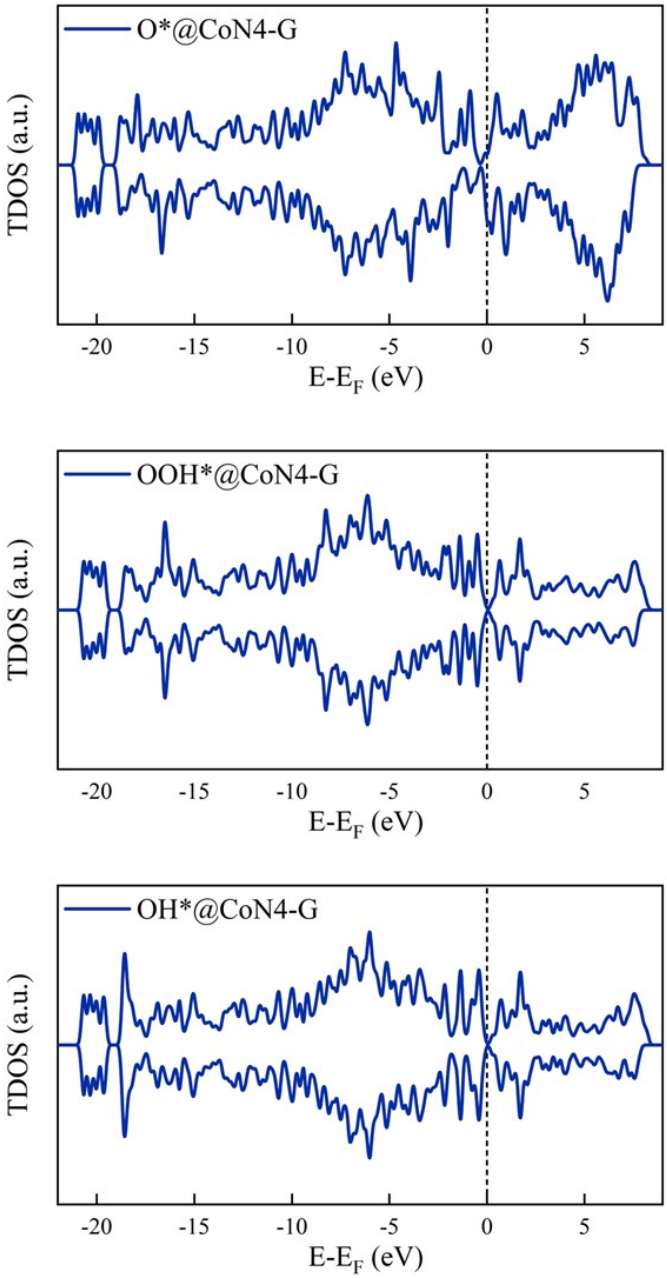

Figure S17. Total density of states (TDOS) of O*, OOH*, and OH* on Co-SAC/NC

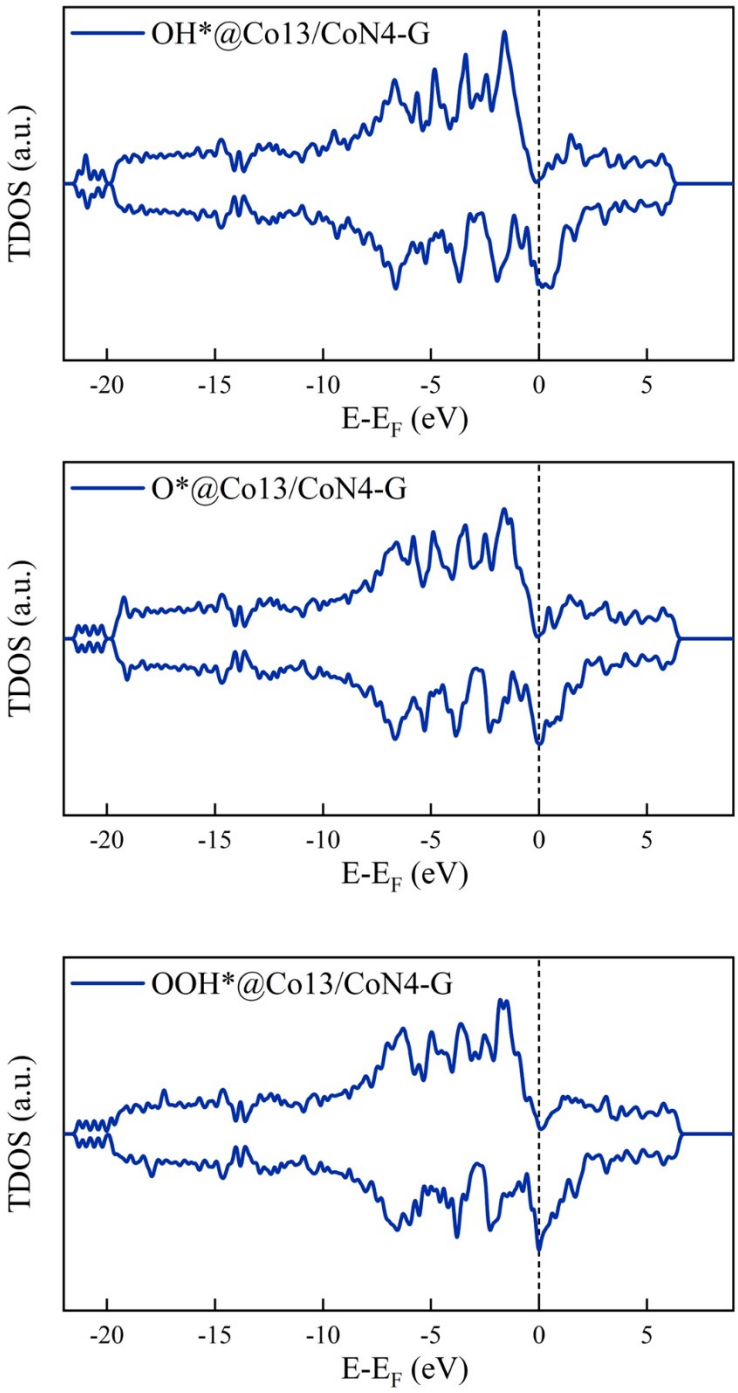

Figure S18. Total density of states (TDOS) of OH*, O*, and OOH* on Co-cluster/NC

In the Supplementary Material, we examined the effects of DFT+*U* (***Figure S19***) and implicit solvent (***Figure S20***) on theoretical calculations. The empirical parameter *U* was set to 3.5 eV for Co, which is taken from previous computational studies [1, 2]. The VASPsol continuum model [3] with water parameters (ε = 78.4) was utilized to depict the solvation status.

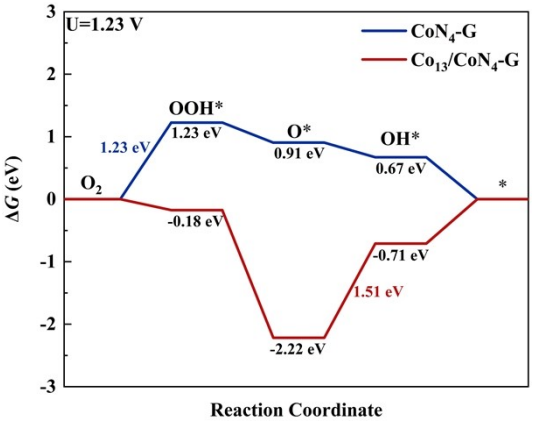

Figure S19**.** DFT+*U*.

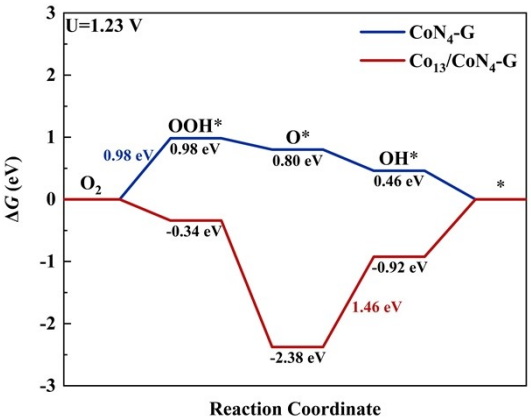

Figure S20**.** Implicit solvation model.

Table S1. The element contents by XPS for different samples.

Samples	XPS (wt%)				ICP (wt%)
	C	N	O	Co	Co
NC	89.57	7.97	2.46	-	-
Co-cluster/NC	85.42	9.92	3.32	1.34	5.41
Co-LC/NC	86.24	9.58	3.66	0.52	1.91
Co-SAC/NC	85.75	9.74	3.25	1.26	4.12

Table S2. EXAFS fitting parameters at the Co K-edge for Co-SAC/NC *(S_0^2=0.724)*.

Sample	Shell	Bond length (Å)	Coordination Number	σ^2 (Å^2)	E_0 shift (eV)	R-factor
Co-SAC/NC	Co-N	1.90±0.02	4.1±0.3	0.010±0.003	-4.9±2.7	0.019
Co-cluster/NC	Co-N	1.78±0.02	2.1±0.4	0.008±0.001	-7.5±4.6	0.005
	Co-O	2.01±0.02	2.9±0.5	0.005±0.003		
	Co-Co	2.46±0.02	0.7±0.1	0.010±0.008		

σ^2, Debye-Waller factor to account for both thermal and structural disorders; E_0 shift (eV), inner potential correction; *R* factor indicates the goodness of the fitting results.

Table S3. Comparative ORR performance of as-prepared catalyst with other reported Co single atom-based ORR catalysts

Catalyst	Half Wave Potential (V)	Relative Current After cycle (%)	Continuously Operation Time (h)	Reference
Co-SAC/NC	0.91	97.4	253	This work
Co $_{SA-AC}$ @SNC	0.86	92.2	10	[4]
Co-SAs@NC	0.82	92.2	10	[5]
Co $_{H}$ SA/NC	0.874	98.6	12.7	[6]
S-Co/N/C	0.86	94.9	100	[7]
Co-SAs/SNPs@NC	0.898	96.51	96	[8]
Co_{40}SAs/AC@NG	0.89	94.5	25	[9]
Co SAs@PNCN	0.851	95.3	12	[10]

Table S4. Comparative TOF and Cdl value of as-prepared catalyst with other reported single atom-based ORR catalysts

Catalyst	TOF (electron^{-1} site^{-1} s^{-1})	Cdl (mF cm^{-2})	Reference
Co-SAC/NC	1.8	72.1	This work
Co_{H} SA/NC	1.33	33.31	[11]
Fe $_{1}$ /NC	/	53.2	[12]
Sn—N/O—C	0.0033	59.5	[13]
Fe-NC-Cor	0.353	/	[14]
$Fe_{sa}Cu_{nc}$/NC	/	38.47	[15]

***Reference*：**

1. Cai, Z.; Bi, Y.; Hu, E.; Liu, W.; Dwarica, N.; Tian, Y.; Li, X.; Kuang, Y.; Li, Y.; Yang, X.-Q.; Wang, H.; Sun, X., Single-crystalline ultrathin Co_3O_4 nanosheets with massive vacancy defects for enhanced electrocatalysis. *Adv. Energy Mater.* **2018,** *8* (3), 1701694.

2. Wang, J.; He, H.; Cai, W.; Yang, C.; Wu, Y.; Zhang, H.; Liu, R.; Cheng, H., Density functional theory optimization of cobalt- and nitrogen-doped graphene catalysts for enhanced oxygen evolution reaction. *Energies* **2023,** *16* (24), 7981.

3. Mathew, K.; Sundararaman, R.; Letchworth-Weaver, K.; Arias, T. A.; Hennig, R. G., Implicit solvation model for density-functional study of nanocrystal surfaces and reaction pathways. *J. Chem. Phys.* **2014,** *140* (8), 084106.

4. Rong, J.; Chen, W.; Gao, E.; Wu, J.; Ao, H.; Zheng, X.; Zhang, Y.; Li, Z.; Kim, M.; Yamauchi, Y.; Wang, C., Design of Atomically Dispersed CoN4 Sites and Co Clusters for Synergistically Enhanced Oxygen Reduction Electrocatalysis. *Small* **2024,** *20* (42), 2402323.

5. Han, X.; Ling, X.; Wang, Y.; Ma, T.; Zhong, C.; Hu, W.; Deng, Y., Generation of nanoparticle, atomic-cluster, and single-atom cobalt catalysts from zeolitic imidazole frameworks by spatial isolation and their use in zinc–air batteries. *Angewandte Chemie* **2019,** *131* (16), 5413-5418.

6. Xie, X.; Peng, H.; Sun, K.; Li, W.; Liang, A.; Ma, G.; Lei, Z.; Xu, Y., A Simultaneous Modulation Strategy to Construct High Dense and Accessible Co-N4 Sites for Promoting Oxygen Reduction Reaction in Zn–Air Battery. *Advanced Functional Materials* **2024**, 2316037.

7. Sun, T.; Zang, W.; Yan, H.; Li, J.; Zhang, Z.; Bu, Y.; Chen, W.; Wang, J.; Lu, J.; Su, C., Engineering the coordination environment of single cobalt atoms for efficient oxygen reduction and hydrogen evolution reactions. *ACS Catalysis* **2021,** *11* (8), 4498-4509.

8. Wang, Z.; Zhu, C.; Tan, H.; Liu, J.; Xu, L.; Zhang, Y.; Liu, Y.; Zou, X.; Liu, Z.; Lu, X., Understanding the synergistic effects of cobalt single atoms and small nanoparticles: enhancing oxygen reduction reaction catalytic activity and stability for zinc-air batteries. *Advanced Functional Materials* **2021,** *31* (45), 2104735.

9. Zhang, M.; Li, H.; Chen, J.; Ma, F. X.; Zhen, L.; Wen, Z.; Xu, C. Y., High-loading Co single atoms and clusters active sites toward enhanced electrocatalysis of oxygen reduction reaction for high-performance Zn–air battery. *Advanced Functional Materials* **2023,** *33* (4), 2209726.

10. Zhang, M.; Li, H.; Chen, J.; Ma, F. X.; Zhen, L.; Wen, Z.; Xu, C. Y., Transition Metal (Co, Ni, Fe, Cu) Single-atom catalysts anchored on 3D nitrogen-doped porous carbon nanosheets as efficient oxygen reduction electrocatalysts for Zn–Air battery. *Small* **2022,** *18* (34), 2202476.

11. Xie, X.; Peng, H.; Sun, K.; Li, W.; Liang, A.; Ma, G.; Lei, Z.; Xu, Y., A Simultaneous Modulation Strategy to Construct High Dense and Accessible Co-N4 Sites for Promoting Oxygen Reduction Reaction in Zn–Air Battery. *Advanced Functional Materials* **2024,** *34* (32), 2316037.

12. Yan, L.; Mao, Y.; Li, Y.; Sha, Q.; Sun, K.; Li, P.; Waterhouse, G. I.;

Wang, Z.; Tian, S.; Sun, X., Sublimation Transformation Synthesis of Dual-Atom Fe Catalysts for Efficient Oxygen Reduction Reaction. *Angewandte Chemie International Edition* **2025,** *64* (1), e202413179.
13. Lin, X.; Zhang, X.; Liu, D.; Shi, L.; Zhao, L.; Long, Y.; Dai, L., Asymmetric Atomic Tin Catalysts With Tailored p-Orbital Electron Structure for Ultra-Efficient Oxygen Reduction. *Advanced Energy Materials* **2024,** *14* (12), 2303740.
14. Li, S.; Liu, M.; Zhang, X.; Chen, X.; Ni, C.; Chen, Y.; Hu, H.; Zheng, K.; Su, H., Low-coordinated Fe− N3 single atom with rapid protonation for boosting oxygen reduction reactions. *Chemical Engineering Journal* **2024,** *502*, 157940.
15. Liang, C.; Han, X.; Zhang, T.; Dong, B.; Li, Y.; Zhuang, Z.; Han, A.; Liu, J., Cu Nanoclusters Accelerate the Rate-Determining Step of Oxygen Reduction on Fe─ N─ C in All pH Range. *Advanced Energy Materials* **2024,** *14* (14), 2303935.